Biomacromolecules

Article

pubs.acs.org/Biomac

Facile Synthesis of Reductively Degradable Biopolymers Using Cystamine Diisocyanate as a Coupling Agent

Xiuxiu Wang, Jian Zhang, Ru Cheng,* Fenghua Meng, Chao Deng, and Zhiyuan Zhong*

Biomedical Polymers Laboratory and Jiangsu Key Laboratory of Advanced Functional Polymer Design and Application, College of Chemistry, Chemical Engineering, and Materials Science, Soochow University, Suzhou, 215123, People's Republic of China

Supporting Information

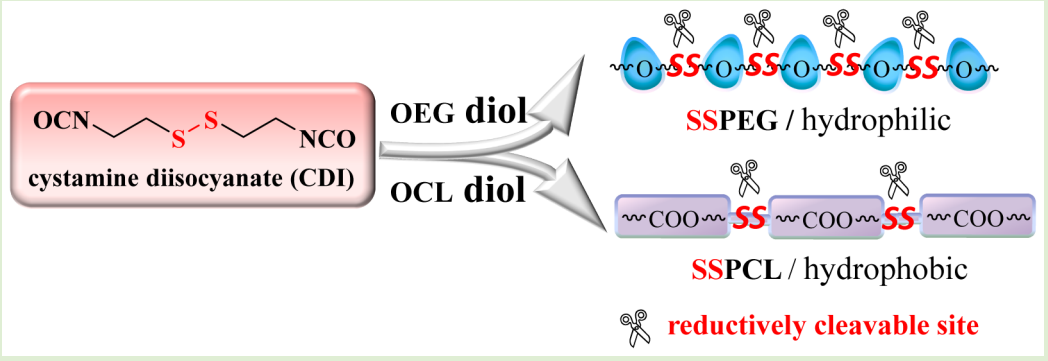

ABSTRACT: Reductively degradable biopolymers have emerged as a unique class of smart biomedical materials. Here, a functional coupling agent, cystamine diisocyanate (CDI), was designed to offer a facile access to reductively degradable biopolymers via polycondensation with various diols. CDI was readily obtained with a decent yield of 46% by reacting cystamine dihydrochloride with triphosgene. The polycondensation of oligo(ethylene glycol) diol (M_n = 0.4 or 1.5 kg/mol) or oligo(ε-caprolactone) diol (M_n = 0.53 kg/mol) with CDI in *N*,*N*-dimethylformamide at 60 °C using dibutyltin dilaurate as a catalyst afforded reductively degradable poly(ethylene glycol) (SSPEG, M_n = 6.2−76.8 kg/mol) or poly(ε-caprolactone) (SSPCL, M_n = 6.8−16.3 kg/mol), in which molecular weights were well controlled by diol/CDI molar ratios. Moreover, PEG-SSPCL-PEG triblock copolymers could be readily prepared by reacting dihydroxyl-terminated SSPCL with PEG-isocyanate derivative. PEG-SSPCL-PEG with an M_n of 5.0−16.3−5.0 kg/mol formed small-sized micelles with an average diameter of about 85 nm in PB buffer. The in vitro release studies using doxorubicin (DOX) as a model drug showed that, in sharp contrast to reduction-insensitive PEG-PCL(HDI)-PEG controls, drug release from PEG-SSPCL-PEG micelles was fast and nearly complete in 24 h under a reductive condition containing 10 mM glutathione. The confocal microscopy experiments in drug-resistant MCF-7 cells (MCF-7/ADR) displayed efficient cytoplasmic DOX release from PEG-SSPCL-PEG micelles. MTT assays revealed that DOX-loaded PEG-SSPCL-PEG micelles were much more potent against MCF-7/ADR cells than reduction-insensitive PEG-PCL(HDI)-PEG controls (IC_{50}: 6.3 vs 55.4 μg/mL). It should further be noted that blank PEG-SSPCL-PEG micelles were noncytotoxic up to a tested concentration of 1 mg/mL. Hence, cystamine diisocyanate appears to be an innovative coupling agent that facilitates versatile synthesis of biocompatible and reductively degradable biopolymers.

INTRODUCTION

Reduction-sensitive nanoparticles have recently emerged as a unique type of nanocarriers for triggered intracellular drug and gene delivery.[1−4] It should be noted that reductively degradable biopolymers, while sufficiently stable under a nonreducing condition (e.g., in blood circulation and in the extracellular milieu), are prone to rapid degradation in the cytosol and nucleus of cancer cells due to the presence of 2−10 mM glutathione (GSH).[5−7] This GSH-triggered fast degradation behavior is distinct from common hydrolytically degradable polymers such as aliphatic polyesters and polycarbonates that gradually degrade in the body, with degradation times ranging from days to weeks to months.[8] The work from different groups has shown that nanocarriers based on reductively degradable biopolymers exhibited markedly enhanced in vitro and in vivo therapeutic effects as compared to their reduction-insensitive counterparts.[9−14]

In the past decade, different synthetic strategies have been employed to furnish reductively degradable biopolymers, which include thiol−disulfide exchange reaction,[15] oxidation of free thiol groups,[16] carbodiimide coupling reaction with disulfide-containing molecules such as cystamine or 3,3′-dithiodipropionic acid,[17−19] Michael-type addition reaction,[20] radical or ring-opening polymerization of disulfide-containing monomers,[21,22] and condensation polymerization of diols with diisocyanates.[23] In particular, condensation polymerization

Received: November 24, 2015
Revised: January 20, 2016
Published: January 26, 2016

DOI: 10.1021/acs.biomac.5b01578
Biomacromolecules 2016, 17, 882−890

approach is appealing in that it is highly robust and versatile, and resulting polymers (i.e., polyurethanes) have excellent stability and biocompatibility. As a matter of fact, polyurethanes (PUs) have been widely used in biomedical fields such as medical implants,[24−27] coatings,[28−30] scaffolds for tissue engineering,[31−35] and drug delivery.[36−39] For example, Tan et al. reported that multiblock PU micelles based on L-lysine ethyl ester diisocyanate (LDI), poly(ε-caprolactone) (PCL) macrodiol, and bis(2-hydroxyethyl) disulfide released about 6-fold more of PTX under a reductive condition (10 mM glutathione) in 48 h than under a nonreductive condition, displaying improved in vitro anticancer effects against HepG2 cells.[40] Ma et al. prepared temperature-triggered redox-degradable poly(ether urethane) nanoparticles based on bis(2-hydroxyethyl) disulfide, hexamethylene diisocyanate (HDI), and PEG that displayed enhanced DOX release into HepG2 cells.[41] Chen et al. reported that DOX-loaded pH and reduction dual-sensitive nanoparticles based on PU of bis-1,4-(hydroxyethyl) piperazine, bis(2-hydroxyethyl) disulfide, and HDI exhibited enhanced growth inhibition of HeLa and HepG2 cells in vitro.[42] We prepared reductively biodegradable α-amino acid-based poly(disulfide urethane)s via polycondensation reaction between two α-amino acid derivatives, disulfide-linked bis(ethyl L-serinate) and LDI.[23] Notably, reduction-responsive PUs are generally prepared by incorporating bis(2-hydroxyethyl) disulfide that might give toxicity issues.

In this paper, we report on the design and development of a novel coupling agent, cystamine diisocyanate (CDI), which offers a facile access to reductively degradable biopolymers via polycondensation with various diols (Scheme 1). Notably, CDI

Scheme 1. Facile Synthesis of Reductively Degradable Biopolymers via Condensation Polymerization of Cystamine Diisocyanate (CDI) with Various Diols

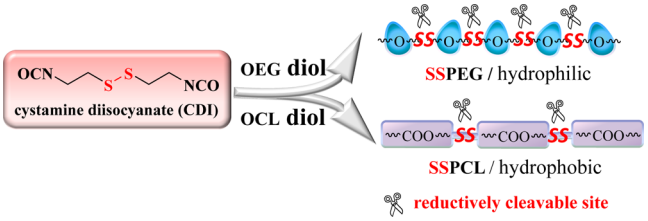

was prepared with a decent yield of 46% by treating cystamine dihydrochloride with triphosgene. Using CDI, we have obtained reductively degradable PCL and PEG, denoted as SSPCL and SSPEG, respectively. Based on SSPCL, we have also prepared reductively degradable PEG-SSPCL-PEG micelles and studied their triggered drug release behavior in vitro and in drug-resistant MCF-7 human breast cancer cells.

2. MATERIALS AND METHODS

2.1. Materials. Methoxy poly(ethylene glycol) (PEG, M_n = 5.0 kg/mol, Fluka), oligo(ethylene glycol) diol (OEG, M_n = 0.4 kg/mol, Sigma-Aldrich; M_n = 1.5 kg/mol, Alfa-Aesar), and oligo(ε-caprolactone) diol (OCL, M_n = 0.53 kg/mol, Sigma-Aldrich) were dried by azeotropic distillation from anhydrous toluene before use. Dichloromethane (DCM) was dried by refluxing over CaH_2 under an argon atmosphere. Triphosgene (BTC, Shanxi Jiaocheng Jingxin Chemical Factory, China) was recrystallized from ethyl acetate prior to use. PEG-LDI was synthesized by treating PEG with excess L-lysine ethyl ester diisocyanate (LDI) according to a previous report.[43] Cystamine dihydrochloride (CDH, 98%, J&K), hydrochloric acid (HCl, 12 M), doxorubicin hydrochloride (DOX·HCl, 99%, Beijing ZhongShuo Pharmaceutical Technology Development Co., Ltd.), 1,4-butanediol (99%, J&K), 2-butene-1, 4-diol (98%, J&K), dibutyltin dilaurate (DBTDL, 97.5%, J&K), glutathione (GSH, 99%, Roche), pyridine (Py, 99.5%, Aladdin), DL-1,4-dithiothreitol (DTT, 99%, J&K), and *N*,*N*-dimethylformamide (DMF, 99%, Alfa Aesar) were used without further purification.

2.2. Characterization. ^{1}H and ^{13}C NMR spectra were recorded on a Unity Inova 400 spectrometer operating at 400 or 600 MHz using $CDCl_3$ or DMSO-d_6 solvent. The molecular weight and polydispersity index (PDI) of copolymers were determined by a Waters 1515 gel permeation chromatograph instrument equipped with MZ-gel SD plus columns (500 Å, 10E3 Å, 10E4 Å) following a differential refractive-index detector (RID 2414). DMF containing 0.05 mol/L LiBr was used as the mobile phase at a flow rate of 0.8 mL/min through the columns at 40 °C. A series of narrow PMMA standards were used for molecular weight calibration. Fourier transform infrared spectrometer (Varian 3600 FTIR) was performed on thermos scientific spectrophotometer with Omnic software for data acquisition and analysis. Each sample for FTIR analysis was prepared by casting the polymer solution (1% (w/v)) in DMF onto a clean potassium bromide disk. The glass transition temperature (T_g) of biopolymers was determined using differential scanning calorimeter (DSC, TA Q200) at a cooling and heating rate of 20 °C/min ranging from −80 to 160 °C with nitrogen flow rate of 25 mL/min. T_g transitions were recorded from the second heating scans using the midpoint infection method. The hydrodynamic size of micelles was determined using dynamic light scattering (DLS). Measurements were carried out at 25 °C by a Zetasizer Nano-ZS (Malvern Instruments) equipped with a 633 nm He−Ne laser using backscattering detection. Transmission electron microscopy (TEM) was performed using a Tecnai G220 TEM operated at an accelerating voltage of 120 kV. The samples were prepared by dropping 10 μL of 0.25 mg/mL micelles suspension on the copper grid followed by staining with 1 wt % phosphotungstic acid.

2.3. Synthesis of Cystamine Diisocyanate (CDI). Under a N_2 atmosphere, cystamine dihydrochloride (CDH; 11.25 g, 50 mmol) was dissolved in 150 mL of DCM, catalytic amount of pyridine (24 mL) was added, and the suspension was cooled to −15 °C in an ice−salt bath. A solution of triphosgene (BTC; 8.9 g, 30 mmol) in 50 mL of DCM was added dropwise by pressure-equalizing dropping funnel over 2 h at −10 °C. The reaction proceeded for another 10 h at −10 °C. The reaction mixture was extracted three times with cold 0.5 M aqueous HCl. The organic phase was dried over anhydrous $MgSO_4$, filtered, and concentrated by rotary evaporation. The product was purified from distillation under reduced pressure. Yield: 46%. FT-IR (cm^{-1}): 2250 (s, *ν*, -N═C═O). ^{1}H NMR (400 MHz, $CDCl_3$, *δ*): 3.63 (t, 4H, -CH_2-N═C═O), 2.88 (t, 4H, -CH_2-S-S-CH_2-). ^{13}C NMR (600 MHz, $CDCl_3$, *δ*): 123.55, 41.58, 39.67. Anal. Calcd for $C_6H_8O_2N_2S_2$: C, 35.28; N, 13.71; H, 3.95. Found: C, 35.06; N, 13.85; H, 3.92. ESI-MS (*m*/*z*): Calcd for $C_6H_8O_2N_2S_2$, 204.0. Found, 203.7.

2.4. Synthesis of SSPEG and SSPCL. SSPEG was prepared by polycondensation reaction between CDI and $OEG_{0.4k}$ or $OEG_{1.5k}$ at varying CDI/OEG molar ratios from 1.03:1 to 1.06:1 to 1.09:1, followed by termination with 1,4-diol. In a typical example, under a N_2 atmosphere, to a solution of CDI (0.210 g, 1.03 mmol) and 0.4k OEG (0.40 g, 1.00 mmol) in DMF (3.6 mL) was added a catalytic amount of DBTDL (7 mg) under stirring. The reaction was allowed to proceed at 60 °C for 24 h. Then, 54 mg (0.6 mmol) of end-capping agent was added, and the reaction was continued at 60 °C for another 12 h. The resulting polymer was isolated by twice precipitation in cold diethyl ether, filtration, and drying in vacuo. Yield: 85%. FT-IR (cm^{-1}): 1600−1800 (s, *ν*, -C═O), 3350 (m, *ν*, -NH-). ^{1}H NMR (400 MHz, DMSO-d_6, *δ* in ppm): 7.38 (s, 2H, -NHCOO-), 4.04 (s, 4H, -NHCOOCH_2-), 3.50 (m, 4H, -CH_2CH_2O-), 3.24 (t, 4H, -CH_2NHCOO-), 2.75 (t, 4H, -CH_2-S-S-CH_2-), 1.55 (s, 2H, HO-CH_2-CH_2CH_2-CH_2-O-), 1.43 (s, 2H, HO-CH_2-CH_2-CH_2-CH_2-O-).

In a similar way, SSPCL was synthesized from polycondensation reaction between CDI and $OCL_{0.53k}$, followed by termination with 2-butene-1,4-diol. Yield: 85%. FT-IR (cm^{-1}): 1600−1800 (s, *ν*, -C═O), 3350 (m, *ν*, -NH-). ^{1}H NMR (400 MHz, DMSO-d_6, *δ*): 7.24 (s, 2H, -NHCOO-), 5.67 (s, 1H, HO-CH═CH-O-), 5.46 (s, 1H, HO-CH═

DOI: 10.1021/acs.biomac.5b01578
Biomacromolecules 2016, 17, 882−890

Table 1. Characterization of Reductively Degradable SSPEG

entry	OEG M_n (kg/mol)	CDI/OEG molar ratio	M_n (kg/mol) ^{1}H NMR[a]	M_n (kg/mol) GPC[b]	PDI[b]	T_g[c] (°C)	yield (%)
1	1.5	1.03:1	76.8	142.4	1.7	−44.7	88.7
2		1.06:1	32.5	72.9	1.6	−46.5	86.8
3		1.09:1	10.4	24.4	1.6	−47.1	85.4
4	0.4	1.03:1	15.3	30.1	1.7	−27.3	87.3
5		1.06:1	12.2	23.6	1.5	−29.5	84.9
6		1.09:1	6.2	15.2	1.4	−36.3	84.3

[a]Determined by ^{1}H NMR end-group analysis. [b]Determined by GPC measurements using DMF as an eluent at a flow rate of 0.8 mL/min (standards: PMMA, 25 °C). [c]Determined by DSC at the second heating scan from −80 to 160 °C at rate of 20 °C/min. T_g is defined as the midpoint of the glass transition.

CH-O-), 4.04−4.11 (t, 4H, -NHCOOCH_2-), 3.91−3.98 (t, 8H, -COOCH_2-), 3.60 (m, 4H, -CH_2OCH_2-), 3.24 (t, 4H, -CH_2NHCOO-), 2.75 (t, 4H, -CH_2-S-S-CH_2-), 2.27 (m, 8H, -CH_2COO-), 1.53 (m, 16H, -COCH$_2$CH_2CH$_2$CH_2CH$_2$O-), 1.29 (m, 8H, -COCH$_2$CH$_2$CH_2CH$_2$CH$_2$O-).

2.5. Reductive Degradation of SSPEG and SSPCL. Under a N_2 atmosphere, 100 mg of SSPEG (Table 1, entry 3 or 5) or SSPCL (Table 2, entry 1) was dissolved in 1 mL of DMF containing 300 mM DTT. The solution was stirred at 37 °C for 4 h and then diluted to 2 mg/mL for GPC measurements.

Table 2. Characterization of Reductively Degradable SSPCL

entry	CDI/OCL molar ratio	M_n (kg/mol) ^{1}H NMR[a]	M_n (kg/mol) GPC[b]	PDI[b]	T_g[c] (°C)	yield (%)
1	1.03:1	16.1	30.0	1.8	−29.7	86.7
2	1.06:1	9.7	16.1	1.7	−32.2	85.2
3	1.09:1	6.8	12.2	1.6	−34.6	84.8

[a]Determined by ^{1}HNMR end-group analysis. [b]Determined by GPC measurements using DMF as an eluent at a flow rate of 0.8 mL/min (standards: PMMA, 25 °C). [c]Determined by DSC at the second heating scan from −80 to 160 °C at rate of 20 °C/min. T_g is defined as the midpoint of the glass transition.

2.6. Synthesis of Reductively Degradable PEG-SSPCL-PEG Triblock Copolymer. PEG-SSPCL-PEG triblock copolymer was prepared by a coupling reaction between PEG-LDI and SSPCL (Table 2, entry 1). Briefly, to a solution of SSPCL diol (0.4 g, 0.025 mmol) in DMF (5 mL) were added PEG-LDI (0.6 g, 0.12 mmol) and a catalytic amount of DBTDL (10 mg). The reaction was allowed to proceed with stirring at 60 °C for 24 h. The resulting copolymer was isolated by twice precipitation from a mixture of diethyl ether and methanol, filtration, and drying in vacuo at room temperature. Yield: 60%. ^{1}H NMR (400 MHz, DMSO-d_6, δ in ppm): SSPCL block: 7.24, 4.04−4.11, 3.91−3.98, 3.60, 3.24, 2.75, 2.27, 1.53, 1.29; PEG-LDI block: 3.51, 3.24, 2.93, 1.17. Similarly, reduction-insensitive PEG-PCL(HDI)-PEG triblock copolymer was prepared by using HDI as a diisocyanate monomer.

2.7. Micelle Formation and Critical Micelle Concentration. Micelles of PEG-SSPCL-PEG and PEG-PCL(HDI)-PEG were prepared under stirring by dropwise addition of 0.8 mL of phosphate buffer (PB, 10 mM, pH 7.4) into 0.2 mL of PEG-SSPCL-PEG or PEG-PCL(HDI)-PEG copolymer solution in DMF (5 mg/mL) followed by extensive dialysis against PB (10 mM, pH 7.4) overnight using a molecular weight cutoff (MWCO) of 3500 at room temperature. The final concentration of micelles was about 0.8 mg/mL.

Pyrene was used as a fluorescence probe for the critical micelle concentration (CMC) determination. The concentration of block copolymer varied from 2.0×10^{-5} to 0.2 mg/mL and the concentration of pyrene was fixed at 1.0 μM. Fluorescence spectra were recorded at an excitation wavelength of 330 nm. Fluorescence emissions at 372 and 383 nm were monitored. The CMC was estimated as the cross-point when extrapolating the intensity ratio I_{372}/I_{383} at low and high concentration regions.

2.8. Change of PEG-SSPCL-PEG Micelle Sizes in Response to 10 mM GSH. Under a N_2 atmosphere, 2.0 mL of PEG-SSPCL-PEG or PEG-PCL(HDI)-PEG micelle dispersion (1 mg/mL) was divided into two aliquots, one in PB (10 mM, pH 7.4) and the other in PB (10 mM, pH 7.4) containing 10 mM GSH. The dispersions were gently shaken at 37 °C. Micelle sizes were monitored at different time intervals by DLS.

2.9. In Vitro Encapsulation of DOX and Reduction Triggered Release of DOX. DOX-loaded micelles were prepared by dropwise addition of 0.8 mL of PB buffer (10 mM, pH 7.4) to a mixture of 0.2 mL of copolymer solution in DMF (5.0 mg/mL) and 30 μL of DOX solution in DMSO (5.0 mg/mL) under stirring at room temperature, followed by extensive dialysis against PB (10 mM, pH 7.4; MWCO 3500) in the dark for 7 h. The dialysis media was changed five times.

To determine drug loading content (DLC), 100 μL of DOX-loaded micelle suspensions was freeze-dried, and then dissolved in 3 mL of DMSO and analyzed with fluorescence spectroscopy. A calibration curve was obtained using DOX/DMSO solutions with different DOX concentrations. To determine the amount of DOX released, calibration curves were run with DOX/corresponding buffer solutions with different DOX concentrations. The emission at 560 nm was recorded. The DLC and drug loading efficiency (DLE) were calculated according to the following formula:

$$\text{DLC(wt\%)} = (\text{wt of loaded drug/total wt of loaded drug and polymer}) \times 100$$

$$\text{DLE(\%)} = (\text{wt of loaded drug/wt of drug in feed}) \times 100$$

The in vitro release of DOX from DOX-loaded PEG-SSPCL-PEG and PEG-PCL(HDI)-PEG micelles was investigated at 37 °C under two different conditions, PB (10 mM, pH 7.4) and PB (10 mM, pH 7.4) containing 10 mM GSH. In order to acquire the sink conditions, drug release studies were performed at low DLC (ca. 5 wt %) and with 0.5 mL of micelle suspension dialysis against 25 mL of appropriate medium (MWCO 12000−14000). At desired time intervals, 5.0 mL of the release medium was taken out and refreshed with an equal volume of fresh medium. As GSH was easy to be oxidized to GSSG, the release experiments were performed under a N_2 atmosphere. The amount of DOX released was determined by fluorescence measurements (excitation at 488 nm, emission at 560 nm). The release experiments were conducted in triplicate. The results presented are the average data.

2.10. MTT Assays. The cytotoxicity of PEG-SSPCL-PEG micelles and PEG-PCL(HDI)-PEG micelles was evaluated using DOX-resistant MCF-7 human breast cancer cell line (MCF-7/ADR) by MTT assays. MCF-7/ADR cells were plated in a 96-well plate (1×10^4 cells/well) in RPMI 1640 media supplemented with 10% fetal bovine serum (FBS), 1% L-glutamine, and antibiotics penicillin (100 IU/mL) and streptomycin (100 μg/mL). After 24 h, the medium was removed and replenished by 80 μL of fresh medium. A 20 μL aliquot of blank PEG-SSPCL-PEG or PEG-PCL(HDI)-PEG micelles were added leading to final micelle concentrations of 0.2, 0.4, 0.6, 0.8, and 1 mg/mL, respectively, and incubated under an atmosphere containing 5% CO_2

DOI: 10.1021/acs.biomac.5b01578
Biomacromolecules 2016, 17, 882−890

Scheme 2. Synthesis of CDI Monomer

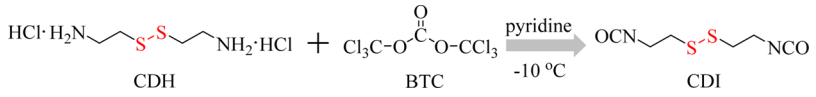

Scheme 3. Synthesis of Reductively Degradable SSPEG and SSPCL[a]

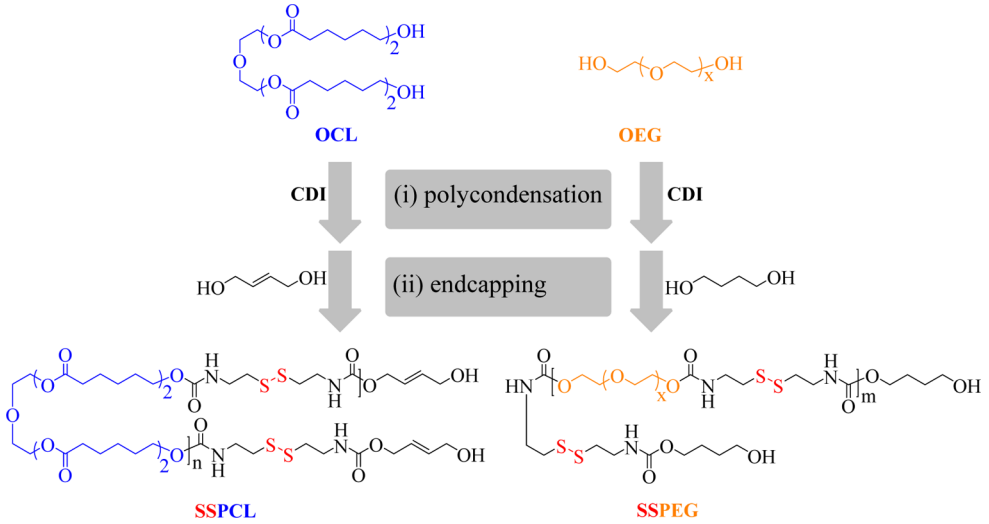

[a]Conditions: (i) DMF, DBTDL, 24 h, 60 °C; (ii) 12 h, 60 °C.

for 48 h at 37 °C. The medium was aspirated and replaced by 100 μL of fresh medium. A 10 μL aliquot of 3-(4,5-dimethylthiazol-2-yl)-2,5-diphenyltetrazolium bromide (MTT) solution (5 mg/mL) was added. The cells were incubated for another 4 h. The medium was carefully aspirated, and the MTT-formazan generated by live cells was dissolved in 150 μL of DMSO, and the absorbance at a wavelength of 570 nm of each well was measured using a microplate reader (Bio-Tek, ELX808 IU). The relative cell viability (%) was determined by comparing the absorbance at 570 nm with control wells containing only cell culture medium.

The antitumor activity of DOX-loaded PEG-SSPCL-PEG or PEG-PCL(HDI)-PEG micelles and free DOX·HCl was also studied by MTT assays in MCF-7/ADR cells, with the exception that instead of blank micelles, 20 μL of DOX-loaded PEG-SSPCL-PEG, PEG-PCL(HDI)-PEG micelles or free DOX·HCl were added resulting in a final DOX concentrations of 0.1, 1, 5, 10, 20, 40, and 80 μg/mL, respectively.

2.11. Confocal Laser Scanning Microscopy (CLSM) Measurements. The cellular uptake and intracellular release behaviors of DOX-loaded PEG-SSPCL-PEG and PEG-PCL(HDI)-PEG micelles were followed with CLSM using MCF-7/ADR cells. MCF-7/ADR cells were plated in a 24-well plate (5×10^4 cells/well) in RPMI 1640 media supplemented with 10% FBS, 1% L-glutamine, and antibiotics penicillin (100 IU/mL) and streptomycin (100 μg/mL) for 24 h. The media were aspirated and replaced by 450 μL of fresh medium. A 50 μL aliquot of DOX-loaded micelles or free DOX·HCl (DOX dosage: 20.0 μg/mL) were added. The cells were incubated with DOX-loaded micelles or free DOX for 8 h at 37 °C in a humidified 5% CO_2 containing atmosphere. The culture medium was removed and the cells were rinsed three times with PBS. The cells were then fixed with 4% paraformaldehyde for 20 min and washed with PBS for three times. The cell nuclei were stained with 4,6-diamidino-2-phenylindole (DAPI, blue) for 20 min and washed with PBS for three times. Fluorescence images of cells were obtained with confocal laser scanning microscope (TCS SP2).

3. RESULTS AND DISCUSSION

3.1. Synthesis and Characterization of CDI Monomer. Novel disulfide-containing diisocyanate monomer, cystamine diisocyanate (CDI), was prepared by treating cystamine dihydrochloride (CDH) with triphosgene (BTC) at −10 °C in DCM in the presence of a catalytic amount of pyridine (Scheme 2), as for synthesis of LDI.[44] CDI was isolated with a good yield of 46% by three times extraction with cold 0.5 M aqueous HCl, drying over anhydrous $MgSO_4$, filtration, rotary evaporation, and distillation under reduced pressure. FT-IR exhibited characteristic peak of isocyanate group at 2250 cm^{-1} (Figure S1A). ^1H NMR revealed that signals assignable to the methylene protons neighboring to the isocyanate and disulfide appeared at δ 3.63 and 2.88, respectively, while resonances attributable to the methylene protons in cystamine at δ 2.71 and 2.96 completely disappeared (Figure S1B). Importantly, signals at δ 3.63 and 2.88 had an integral ratio close to 1:1, in line with quantitative conversion of amino function into isocyanate. ^{13}C NMR detected three carbon signals at δ 123.55, 41.58, and 39.67, attributable to the carbons of isocyanate and two methylene carbons, respectively (Figure S1C). The chemical structure of CDI was further confirmed by ESI mass spectroscopy and elemental analysis.

3.2. Synthesis of Reductively Degradable SSPEG and SSPCL. The polycondensation reaction between CDI and OEG (M_n = 0.4 and 1.5 kg/mol) was carried out at varying CDI/OEG molar ratios ranging from 1.03/1 to 1.06/1 to 1.09/1 at 60 °C for 24 h in DMF using DBTDL as a catalyst, followed by end-capping with 1,4-butanediol (Scheme 3). SSPEG polymers were obtained with 84.3−88.7% yields (Table 1). FT-IR spectrum of SSPEG revealed absorption band characteristic of urethane stretch at 3350 cm^{-1} (Figure S3). ^1H NMR showed besides characteristic signals of OEG at δ 3.50 also resonances at δ 1.55 and 1.43 assignable to the terminal 1,4-butane diol moieties, δ 7.38 to the urethane protons, as well as δ 3.24 and 2.75 to the CDI moieties (Figure 2A). The M_n of resulting SSPEG could be determined by comparing the integrals at δ 2.75 and 3.50 to 1.55. The results showed that with decreasing

DOI: 10.1021/acs.biomac.5b01578
Biomacromolecules 2016, 17, 882−890

CDI/OEG molar ratios from 1.09 to 1.03, the M_n of SSPEG increased from 10.4 to 32.5 to 76.8 kg/mol and from 6.2 to 12.2 to 15.3 kg/mol, for 1.5 k and 0.4 k OEG, respectively (Table 1). The chemical structure of SSPEG was further confirmed by ^{13}C NMR (Figure S4). GPC measurements showed that thus obtained SSPEG had moderate polydispersity indices of 1.4−1.7 and M_n values decreased in parallel with those determined by ^{1}H NMR end-group analyses. The higher M_n (GPC) as compared to M_n (^{1}H NMR) is likely because PMMA was used to calibrate the GPC columns. Notably, the M_n (^{1}H NMR) data fitted well with those calculated based on the Carothers equation, assuming 87−100% monomer conversion. It should further be noted that accurate weighing of monomers though is of critical importance in condensation polymerization is not easy to accomplish in practice. The slight deviation of M_n (^{1}H NMR) data from the calculated ones could be due to differences in monomer conversion as well as altered monomer ratios. Thermal analyses indicated that all SSPEG polymers were amorphous, in which with decreasing M_n, T_g of SSPEG decreased from −44.7 to −47.1 °C for 1.5 k OEG and from −27.3 to −36.3 °C for 0.4 k OEG (Table 1). In general, SSPEG polymers based on 1.5 k OEG had a lower T_g than those based on 0.4 k OEG. Similar results have been observed by Wang's group that T_g of poly(ether urethane)s increased from −51.8 to −27.4 with decreasing of the molecular weight of OEG from 1.5 k to 0.6 k.[45] Solubility tests indicated that SSPEG was soluble in various organic solvents, such as tetrahydrofuran, dimethyl sulfoxide, acetone, DCM, DMF, ethanol, and methanol. SSPEG based on 1.5 k OEG was soluble in water, with a hydrodynamic size of about 10 nm, as revealed by DLS.

SSPCL was synthesized as for SSPEG except that 2-butene-1,4-diol was used as an end-capping agent. The yields ranged from 84.8% to 86.7% (Table 2). The polymerization was monitored by FTIR, which revealed gradual disappearance of the characteristic absorbance of isocyanate at 2250 cm^{-1} over time (Figure 1). ^{1}H NMR showed signals assignable to OCL

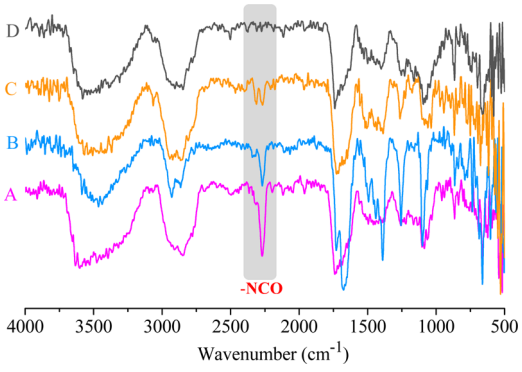

Figure 1. FT-IR spectra of OCL and CDI condensation polymerization mixture at 0 (A), 8 (B), and 24 h (C) and after end-capping with 2-butene-1,4-diol (D).

moieties (δ 3.98, 3.91, 3.60, 2.27, 1.53, 1.29), vinyl protons of terminal 2-butene-1,4-diol moieties at δ 5.67 and 5.46 and urethane protons at δ 7.38 (Figure 2B). The M_n of resulting SSPCL could be determined by comparing the integrals at δ 2.75 (methylene protons of CDI moieties) and 1.53 (methylene protons of OCL moieties) to 5.67 (vinyl protons). The results showed that SSPCL had M_n values varying from 16.3 to 9.7 to 6.8 kg/mol, which decreased in parallel with

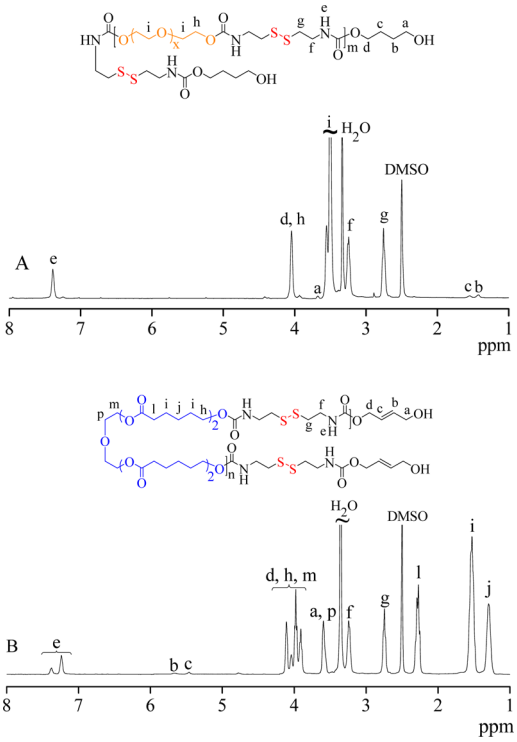

Figure 2. ^{1}H NMR spectra (400 MHz, DMSO-d_6) of SSPEG (Table 1, entry 2) (A) and SSPCL (Table 2, entry 1) (B).

increasing CDI/OCL molar ratios. The structure of SSPCL was also confirmed by ^{13}C NMR (Figure S5). GPC displayed that SSPCL had a unimodal distribution with a moderate PDI of 1.6 to 1.8 and M_n values ranging from 12.2 to 30.0 kg/mol depending on CDI/OCL molar feed ratios. M_n determined by GPC increased in good accordance with that determined by ^{1}H NMR end group analyses. The M_n (^{1}H NMR) data fitted well with those calculated based on the Carothers equation assuming 93−97% monomer conversion. The somewhat lower molecular weight of SSPCL could also be due to the fact that besides inaccurate weighing of monomers, OCL monomer is not precisely defined. Thermal analyses indicated that thus obtained SSPCL was amorphous with T_g ranging from −29.8 to −34.7 °C, which increased with increasing M_n (Table 2).

To verify the reductive degradation property, SSPEG and SSPCL following 3 h incubating with 300 mM DTT in DMF was subject to GPC measurements. The results showed that M_n of SSPEG prepared from 1.5 k OEG (Table 1, entry 3) declined from 24.4 to 3.4 kg/mol, and that of SSPCL (Table 2, entry 1) declined from 16.1 to 1.0 kg/mol (Figure 3), confirming fast and complete cleavage of the disulfide bonds in the backbone.

3.3. Preparation of Reductively Degradable PEG-SSPCL-PEG Triblock Copolymer and Micelles. SSPCL with an M_n of 16.1 kg/mol and a PDI of 1.8 (Table 2, entry 1) was chosen to prepare PEG-SSPCL-PEG triblock copolymer. PEG-SSPCL-PEG was obtained by reacting SSPCL with 1.5-fold excess of PEG-LDI (M_n = 5.0 kg/mol) in DMF at 60 °C in the presence of a catalytic amount of DBTDL for 24 h (Scheme 4). The excess PEG was removed by precipitation in a diethyl ether/methanol mixture. ^{1}H NMR detected besides signals assignable to SSPCL block also resonances owing to the methyl and methylene protons of PEG at δ 3.24 and 3.51 and

DOI: 10.1021/acs.biomac.5b01578
Biomacromolecules 2016, 17, 882−890

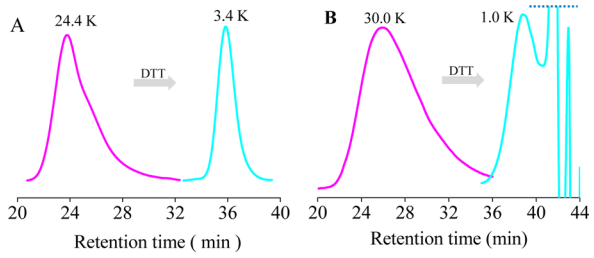

Figure 3. GPC chromatograms of SSPEG (Table 1, entry 3) (A) and SSPCL (Table 2, entry 1) (B) before and after 3 h degradation by 300 mM DTT.

methylene protons of LDI moiety at δ 2.93 and 1.17 (Figure 4). The integral ratio of signals of the methylene protons of PEG-LDI nearby the urethane bond (δ 2.93) and methylene protons of SSPCL neighboring to disulfide bond (δ 2.75) was close to the theoretical value of 1:23, in line with that PEG and SSPCL blocks had a molar ratio of 2:1. In accordance, PEG-SSPCL-PEG had an M_n of 5.0−16.1−5.0 kg/mol. GPC curve revealed a unimodal distribution with a low M_w/M_n of 1.3 (Figure S6), corroborating successful synthesis of PEG-SSPCL-PEG triblock copolymer. We have also prepared reduction-insensitive PEG-PCL(HDI)-PEG triblock copolymer with an M_n of 5.0−15.5−5.0, as calculated from ^{1}H NMR (Figure S7), by using HDI to replace CDI.

Micelles were prepared from PEG-SSPCL-PEG triblock copolymer by solvent exchange method. Dynamic light scattering (DLS) measurements showed that PEG-SSPCL-PEG formed micelles with an average diameter of about 85 nm and a low polydispersity (PDI) of 0.11 in PB (10 mM, pH 7.4; Figure 5A). TEM micrograph of PEG-SSPCL-PEG micelles revealed a homogeneous distribution of spherical nanoparticles with sizes in accordance with those determined by DLS. CMC measurements using pyrene as a fluorescence probe showed that PEG-SSPCL-PEG triblock copolymer had a low CMC value of 5.5 mg/L. Under the same conditions, PEG-PCL(HDI)-PEG copolymers formed micelles with an average size of about 90 nm in PB (10 mM, pH 7.4) and a low PDI of 0.13 (Figure S8). PEG-PCL(HDI)-PEG exhibited an CMC value of 3.3 mg/L. The size change of PEG-SSPCL-PEG micelles in response to 10 mM GSH was followed by DLS measurements. The results showed that PEG-SSPCL-PEG micelles underwent rapid and remarkable swelling in the presence of 10 mM GSH, in which average size increased from

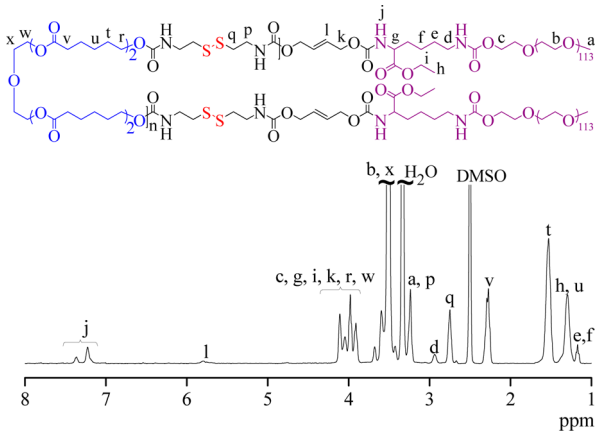

Figure 4. ^{1}H NMR spectrum (400 MHz, DMSO-d_6) of PEG-SSPCL-PEG triblock copolymer.

about 85 to 110 nm in 10 h and reached over 1000 nm in 24 h (Figure 5B). In contrast, little change of PEG-SSPCL-PEG micelles size was observed over 24 h at pH 7.4 under otherwise the same conditions, implying that PEG-SSPCL-PEG micelles have adequate aqueous stability. These results corroborate fast responsivity of PEG-SSPCL-PEG micelles to the cytoplasmic reductive environment, similar to our previous reports for reductively degradable SSPEA-Gal nanoparticles.[46]

3.4. Triggered Drug Release and Antitumor Activity.

DOX was used as a model anticancer drug to evaluate the drug encapsulation and release behaviors of PEG-SSPCL-PEG and PEG-PCL(HDI)-PEG micelles. DOX-loaded micelles were prepared via the solvent exchange method. At a theoretical drug loading content (DLC) of 15 wt %, both PEG-SSPCL-PEG and PEG-PCL(HDI)-PEG micelles showed a DLC of about 8 wt % and drug loading efficiency (DLE) of about 58.0% (Table 3). The in vitro drug release studies were carried out at a low micelle concentration of 0.2 mg/mL at 37 °C using a dialysis tube (MWCO 12000) in PB (10 mM, pH 7.4) in the presence or absence of 10 mM GSH. The accumulative drug release profiles as a function of time are plotted in Figure 6. Remarkably, the results showed that PEG-SSPCL-PEG micelles released DOX rapidly in the presence of 10 mM GSH. For example, about 57% DOX was released in 6 h and nearly 90% of DOX release was observed after 24 h. In contrast, less than 30% drug was released within 24 h for reduction-insensitive PEG-PCL(HDI)-PEG micelles under the same condition as

Scheme 4. Synthesis of the Reductively Degradable PEG-SSPCL-PEG Triblock Copolymer

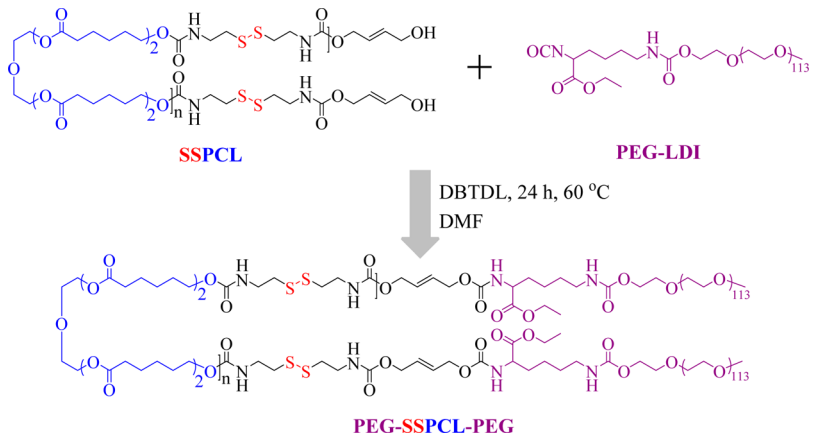

DOI: 10.1021/acs.biomac.5b01578
Biomacromolecules 2016, 17, 882−890

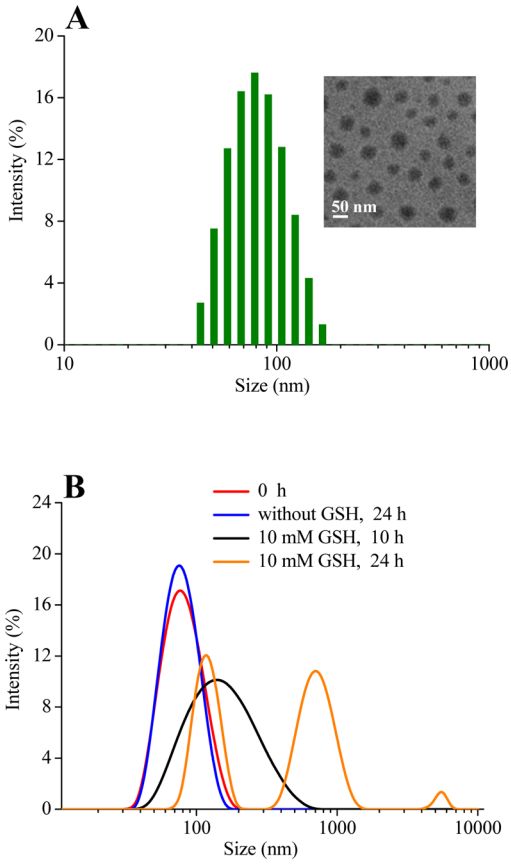

Figure 5. Size distribution of PEG-SSPCL-PEG micelles determined by DLS and TEM (A) and change of micelle sizes in response to 10 mM GSH (B).

Table 3. Characterization of DOX-Loaded PEG-SSPCL-PEG and PEG-PCL(HDI)-PEG Micelles

micelles	size[a]	PDI[a]	DLC[b] (wt %)	DLE (%)	CMC[c] (mg/L)
PEG-SSPCL-PEG	94	0.11	8.1	58.4	5.1
PEG-PCL(HDI)-PEG	82	0.13	8.0	57.9	2.3

[a]Determined by DLS using Zetasizer Nano-ZS (Malvern Instruments) at 25 °C in PB buffer. [b]Determined by UV−vis. [c]Determined by fluorescence. Pyrene was used as fluorescence probe.

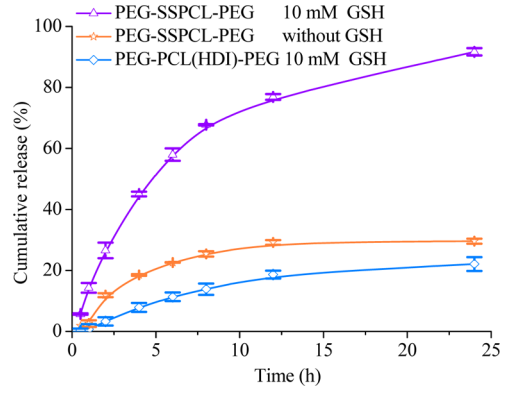

Figure 6. In vitro DOX release from DOX-loaded PEG-SSPCL-PEG micelles and PEG-PCL(HDI)-PEG micelles in PB (10 mM, pH 7.4) in the presence or absence of GSH at 37 °C.

well as for PEG-SSPCL-PEG micelles under a nonreductive condition.

The cytotoxicity of PEG-SSPCL-PEG micelles and antitumor activity of DOX-loaded micelles were investigated by MTT assays in drug-resistant MCF-7/ADR cells. The results revealed that PEG-SSPCL-PEG micelles were noncytotoxic even at a high concentration of 1.0 mg/mL (Figure 7A), confirming that

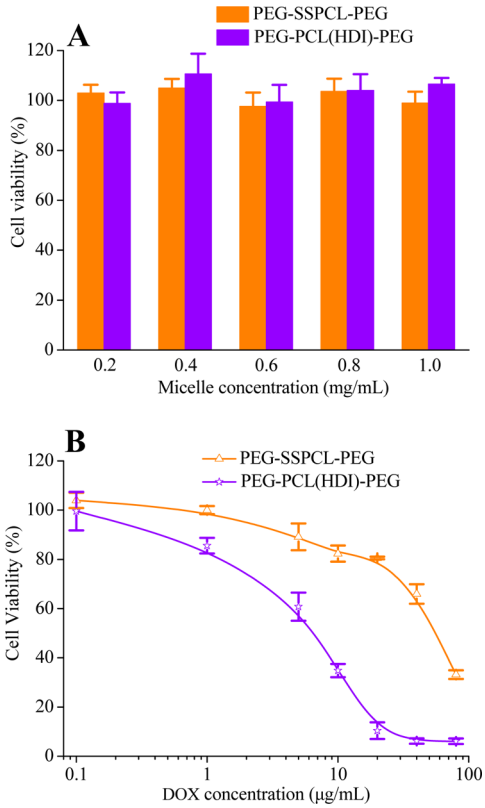

Figure 7. MTT assays in MCF-7/ADR cells. (A) Blank PEG-SSPCL-PEG and PEG-PCL(HDI)-PEG micelles; and (B) DOX-loaded PEG-SSPCL-PEG micelles and DOX-loaded PEG-PCL(HDI)-PEG micelles. Results are presented as the mean ± SD (n = 4).

PEG-SSPCL-PEG copolymers have good biocompatibility. Notably, DOX-loaded PEG-SSPCL-PEG micelles caused effective growth inhibition of MCF-7/ADR cells (Figure 7B). The half-maximal inhibitory concentration (IC_{50}) of DOX-loaded PEG-SSPCL-PEG micelles was determined to be 6.3 μg DOX equiv/mL, which is almost 9× lower than that for corresponding PEG-PCL(HDI)-PEG micelles (reduction-insensitive control). This effective reversal of drug resistance is most probably due to a combination of cellular uptake via the endocytosis mechanism and fast intracellular drug release.[47−49]

CLSM was employed to study the intracellular DOX release from PEG-SSPCL-PEG micelles in MCF-7/ADR cells. As shown in Figure 8, strong DOX fluorescence was detected in the cytoplasm and perinuclei regions of MCF-7/ADR cells following 8 h incubation, corroborating a high intracellular free DOX level. In contrast, little DOX fluorescence was observed in MCF-7/ADR cells following 8 h treatment with DOX-loaded PEG-PCL(HDI)-PEG micelles and free DOX·HCl. These results support that reductively degradable micelles based on PEG-SSPCL-PEG mediate highly efficient intracellular drug release. It should further be noted that the selectivity and

DOI: 10.1021/acs.biomac.5b01578
Biomacromolecules 2016, 17, 882−890

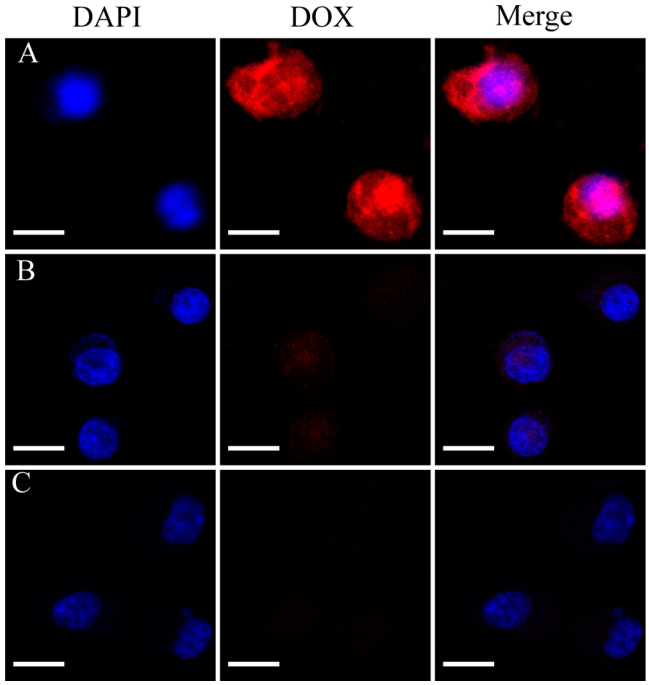

Figure 8. CLSM images of MCF-7/ADR cells following 8 h incubation with (A) DOX-loaded PEG-SSPCL-PEG micelles, (B) DOX-loaded PEG-PCL(HDI)-PEG micelles, or (C) free DOX·HCl (DOX dosage: 20 μg/mL). For each panel, the images show cell nuclei stained by DAPI (blue), DOX fluorescence in cells (red), and overlays of the two images. The scale bars correspond to 15 μm in all the images.

antitumor activity of these systems can further be improved by installing a specific targeting ligand.

CONCLUSIONS

We have demonstrated for the first time that cystamine diisocyanate can be readily prepared and used as a novel functional monomer for the versatile development of reductively degradable biopolymers via condensation polymerization. The molecular weights of resulting biopolymers are controlled by isocyanate/hydroxyl molar ratios. Notably, micelles based on reductively degradable PEG-SSPCL-PEG triblock copolymer exhibit low cytotoxicity and glutathione-triggered drug release behavior in vitro. Furthermore, doxorubicin-loaded PEG-SSPCL-PEG micelles show efficient intracellular drug release and significantly improved antitumor effect toward drug-resistant MCF-7 cells as compared to their reduction-insensitive counterparts and free doxorubicin. Based on cystamine diisocyanate monomer, reductively degradable biopolymers with vastly different structures and properties can be obtained. These reductively degradable biopolymers with easy synthesis, good biocompatibility, and triggered drug release provide an advanced platform for controlled drug delivery.

ASSOCIATED CONTENT

Supporting Information

The Supporting Information is available free of charge on the ACS Publications website at DOI: 10.1021/acs.biomac.5b01578.

FT-IR, ^{1}H NMR, and ^{13}C NMR spectra of CDI; ^{1}H NMR spectrum of CDH; FT-IR spectra of SSPEG and SSPCL; ^{13}C NMR spectra of SSPEG and SSPECL; GPC chromatograms of SSPCL and PEG-SSPCL-PEG; ^{1}H NMR spectrum of PEG-PCL(HDI)-PEG; and size distribution of PEG-PCL(HDI)-PEG micelles determined by DLS and TEM (PDF).

AUTHOR INFORMATION

Corresponding Authors

*Tel./Fax: +86-512-65880098. E-mail: rcheng@suda.edu.cn.
*E-mail: zyzhong@suda.edu.cn.

Notes

The authors declare no competing financial interest.

ACKNOWLEDGMENTS

This work was supported by the National Natural Science Foundation of China (NSFC 51103093 and 51373113), the National Science Fund for Distinguished Young Scholars (51225302), the Natural Science Foundation of Jiangsu Province (BK201321510), a Project Funded by the Priority Academic Program Development of Jiangsu Higher Education Institutions, and the Project of Science and Technology of Suzhou (SYG201331).

REFERENCES

(1) Mura, S. N. J.; Couvreur, P. *Nat. Mater.* **2013**, *12*, 991−1003.
(2) Jhaveri, A. D. P.; Torchilin, V. *J. Controlled Release* **2014**, *190*, 352−370.
(3) Huo, M.; Yuan, J. Y.; Tao, L.; Wei, Y. *Polym. Chem.* **2014**, *5*, 1519−1528.
(4) Cheng, R.; Feng, F.; Meng, F. H.; Deng, C.; Feijen, J.; Zhong, Z. Y. *J. Controlled Release* **2011**, *152*, 2−12.
(5) Phillips, D. J.; Gibson, M. I. *Antioxid. Redox Signaling* **2014**, *21*, 786−803.
(6) Brulisauer, L.; Gauthier, M. A.; Leroux, J. C. *J. Controlled Release* **2014**, *195*, 147−154.
(7) Meng, F. H.; Hennink, W. E.; Zhong, Z. Y. *Biomaterials* **2009**, *30*, 2180−2198.
(8) Ahmed, F.; Discher, D. E. *J. Controlled Release* **2004**, *96*, 37−53.
(9) Jia, L.; Cui, D.; Bignon, J.; Cicco, A. D.; Wdzieczak-Bakala, J.; Liu, J. M.; Li, M. H. *Biomacromolecules* **2014**, *15*, 2206−2217.
(10) Yu, S. J.; Ding, J. X.; He, C. L.; Cao, Y.; Xu, W. G.; Chen, X. S. *Adv. Healthcare Mater.* **2014**, *3*, 752−760.
(11) Xu, P. F.; Yu, H. J.; Zhang, Z. W.; Meng, Q. S.; Sun, H. P.; Chen, X. Z.; Yin, Q.; Li, Y. P. *Biomaterials* **2014**, *35*, 7574−7587.
(12) Ryu, J. H.; Chacko, R. T.; Jiwpanich, S.; Bickerton, S.; Babu, R. P.; Thayumanavan, S. *J. Am. Chem. Soc.* **2010**, *132*, 17227−17235.
(13) Zhong, Y. N.; Zhang, J.; Cheng, R.; Deng, C.; Meng, F. H.; Xie, F.; Zhong, Z. Y. *J. Controlled Release* **2015**, *205*, 144−154.
(14) Chen, W.; Zou, Y.; Jia, J. N.; Meng, F. H.; Cheng, R.; Deng, C.; Feijen, J.; Zhong, Z. Y. *Macromolecules* **2013**, *46*, 699−707.
(15) Sun, H. L.; Guo, B. N.; Cheng, R.; Meng, F. H.; Liu, H. Y.; Zhong, Z. Y. *Biomaterials* **2009**, *30*, 6358−6366.
(16) Sun, R.; Luo, Q. J.; Gao, C.; Wang, Y.; Gao, L. L.; Du, H.; Huang, Y.; Li, X. D.; Shen, Z. Q.; Zhu, W. P. *Polym. Chem.* **2014**, *5*, 4879−4883.
(17) Chen, W.; Zheng, M.; Meng, F. H.; Cheng, R.; Deng, C.; Zhong, Z. Y. *Biomacromolecules* **2013**, *14*, 1214−1222.
(18) Lv, S. X.; Tang, Z. H.; Zhang, D. W.; Song, W. T.; Li, M. Q.; Lin, J.; Liu, H. Y.; Chen, X. S. *J. Controlled Release* **2014**, *194*, 220−227.
(19) Hu, Y. W.; Du, Y. Z.; Liu, N.; Liu, X.; Meng, T. T.; Cheng, B. L.; He, J. B.; You, J.; Yuan, H.; Hu, F. Q. *J. Controlled Release* **2015**, *206*, 91−100.
(20) Chen, W.; Zou, Y.; Meng, F. H.; Cheng, R.; Deng, C.; Feijen, J.; Zhong, Z. Y. *Biomacromolecules* **2014**, *15*, 900−907.

DOI: 10.1021/acs.biomac.5b01578
Biomacromolecules 2016, 17, 882−890

(21) Khorsand, B.; Lapointe, G.; Brett, C.; Oh, J. K. *Biomacromolecules* **2013**, *14*, 2103−2111.
(22) Liu, J. Y.; Liu, W. G.; Weitzhandler, I.; Bhattacharyya, J.; Li, X. H.; Wang, J.; Qi, Y. Z.; Bhattacharjee, S.; Chilkoti, A. *Angew. Chem., Int. Ed.* **2015**, *54*, 1002−1006.
(23) Lu, W. T.; Wang, X. X.; Cheng, R.; Deng, C.; Meng, F. H.; Zhong, Z. Y. *Polym. Chem.* **2015**, *6*, 6001−6010.
(24) Singhal, P.; Small, W.; Cosgriff-Hernandez, E.; Maitland, D. J.; Wilson, T. S. *Acta Biomater.* **2014**, *10*, 67−76.
(25) Styan, K. E.; Martin, D. J.; Simmons, A.; Poole-Warren, L. A. *Acta Biomater.* **2012**, *8*, 2243−2253.
(26) Yoshii, T.; Dumas, J. E.; Okawa, A.; Spengler, D. M.; Guelcher, S. A. *J. Biomed. Mater. Res., Part B* **2012**, *100*, 32−40.
(27) Bergmeister, H.; Seyidova, N.; Schreiber, C.; Strobl, M.; Grasl, C.; Walter, I.; Messner, B.; Baudis, S.; Frohlich, S.; Marchetti-Deschmann, M.; Griesser, M.; di Franco, M.; Krssak, M.; Liska, R.; Schima, H. *Acta Biomater.* **2015**, *11*, 104−113.
(28) Wang, C. H.; Ma, C. F.; Mu, C. D.; Lin, W. *Langmuir* **2014**, *30*, 12860−12867.
(29) Sharmin, E.; Fahmina Zafara, F.; Akram, D.; Ahmada, S. *Prog. Org. Coat.* **2013**, *76*, 541−547.
(30) Wynne, J. H.; Fulmer, P. A.; McCluskey, D. M.; Mackey, N. M.; Buchanan, J. P. *ACS Appl. Mater. Interfaces* **2011**, *3*, 2005−2011.
(31) Perez, R. A.; Won, J. E.; Knowles, J. C.; Kim, H. W. *Adv. Drug Delivery Rev.* **2013**, *65*, 471−496.
(32) Pascual-Gil, S.; Garbayo, E.; Diaz-Herraez, P.; Prosper, F.; Blanco-Prieto, M. J. *J. Controlled Release* **2015**, *203*, 23−38.
(33) McBane, J. E.; Sharifpoor, S.; Cai, K. H.; Labow, R. S.; Santerre, J. P. *Biomaterials* **2011**, *32*, 6034−6044.
(34) Jia, L.; Prabhakaran, M. P.; Qin, X. H.; Kai, D.; Ramakrishna, S. *J. Mater. Sci.* **2013**, *48*, 5113−5124.
(35) Niu, Y. Q.; Chen, K. C.; He, T.; Yu, W. Y.; Huang, S. W.; Xu, K. T. *Biomaterials* **2014**, *35*, 4266−4277.
(36) Zhou, L. J.; Yu, L. Q.; Ding, M. M.; Li, J. H.; Tan, H.; Wang, Z. G.; Fu, Q. *Macromolecules* **2011**, *44*, 857−864.
(37) Morral-Ruiz, G.; Melgar-Lesmes, P.; Solans, C.; Garcia-Celma, M. J. *J. Controlled Release* **2013**, *171*, 163−171.
(38) Cao, W.; Gu, Y. W.; Meineck, M.; Li, T. Y.; Xu, H. P. *J. Am. Chem. Soc.* **2014**, *136*, 5132−5137.
(39) Rosenbauer, E. M.; Wagner, M.; Musyanovych, A.; Landfester, K. *Macromolecules* **2010**, *43*, 5083−5093.
(40) He, X. L.; Ding, M. M.; Li, J. H.; Tan, H.; Fu, Q.; Li, L. *RSC Adv.* **2014**, *4*, 24736−24746.
(41) Wang, Y. Y.; Wu, G. L.; Li, X. M.; Chen, J. T.; Wang, Y. N.; Ma, J. B. *J. Mater. Chem.* **2012**, *22*, 25217−25226.
(42) Yu, S. J.; He, C. L.; Ding, J. X.; Cheng, Y. L.; Song, W. T.; Zhuang, X. L.; Chen, X. S. *Soft Matter* **2013**, *9*, 2637−2645.
(43) Jo, S.; Park, K. *Biomaterials* **2000**, *21*, 605−616.
(44) Zhang, Y.; Zhuo, R. X. *Biomaterials* **2005**, *26*, 6736−6742.
(45) Lu, H. X.; Sun, P. Y.; Zheng, Z.; Yao, X.; Wang, X. L.; Chang, F. C. *Polym. Degrad. Stab.* **2012**, *97*, 661−669.
(46) Lv, J. L.; Sun, H. L.; Zou, Y.; Meng, F. H.; Dias, A. A.; Hendriks, M.; Feijen, J.; Zhong, Z. Y. *Biomater. Sci.* **2015**, *3*, 1134−1146.
(47) Ren, Y.; Wang, R. R.; Liu, Y.; Guo, H.; Zhou, X.; Yuan, X. B.; Liu, C. Y.; Yian, J. G.; Yin, H. F.; Wang, Y. S.; Zhang, N. *Biomaterials* **2014**, *35*, 2462−2470.
(48) Yu, H. J.; Cui, Z. R.; Yu, P. C.; Guo, C. Y.; Feng, B.; Jiang, T. Y.; Wang, S. L.; Yin, Q.; Zhong, D. F.; Yang, X. L.; Zhang, Z. W.; Li, Y. P. *Adv. Funct. Mater.* **2015**, *25*, 2489−2500.
(49) Shi, Q.; Zhang, L.; Liu, M. Y.; Zhang, X. L.; Zhang, X. J.; Xu, X. Q.; Chen, S.; Li, X. H.; Zhang, J. X. *Biomaterials* **2015**, *67*, 169−182.

DOI: 10.1021/acs.biomac.5b01578
Biomacromolecules 2016, 17, 882−890